



# THE STRATEGIC ROLE OF $TiO_2$ BASED PHOTOCATALYSTS IN DYE DEGRADATION STUDIES: A SHORT REVIEW

M.SudhaMaheswari<sup>1</sup>, JalajakshiTammineni<sup>2</sup>, Dilip Kumar Behara<sup>3</sup>

<sup>1,2,3</sup>Department of Chemical Engineering, JNTUA College of Engineering, Anantapuramu (India)

## ABSTRACT

Synthetic dyes have extensive application in textile, leather, paper, food, and agricultural research and therefore have large-scale production. However, they cause considerable environmental pollution and serious health-risk factors. Therefore, it is essential to remove dyes completely or treat the streams containing dye effluents with more efficient and cost effective technologies. In this regard,  $TiO_2$  based photocatalysis has received considerable interest due to its abundant availability, high stable, inert cum non-toxic, and high redox potential for degrading the dye. This review focuses on a) various mechanisms for photo catalytic dye degradation, b) strategies/methodologies for enhancing  $TiO_2$  photocatalytic properties and finally c) some typical issues, which are unaddressed in the context of photocatalytic dye degradation using  $TiO_2$  based catalysts.

**Keywords:** catalysts ,effluents,dye degradation  $TiO_2$  based photocatalysis, effective technologies.

## I. INTRODUCTION

Textile industry serves major fraction of income and strongly depend on economic development of any country. However, the untreated liquid effluents containing dyes from the outlet of these industries cause very severe environmental pollution problems. Therefore, it is inevitable to treat the dye effluent streams before they release into water bodies. Dye degradation treatment techniques have been classified as physical, chemical, and biological.

Physical techniques such as activated carbon, adsorption, reverse osmosis etc. causes secondary pollution to the environment as they require further treatment of solid-wastes, finally this adds additional cost to the process. Chemical processes involves adsorption on organic or inorganic matrices, ozonation, chemical oxidation processes, advanced oxidation processes such as Fenton and photo-Fenton catalytic reactions,  $H_2O_2$ /UV processes and photo degradation through photocatalysis. Toxic unstable metabolites resulted from these processes imparts adverse effects on human health [1-7].

Biological techniques involving aerobic and anaerobic conditions are known to be ineffective for degradation of dyes due to higher molecular weight of "coloured" substances [8]. Moutaouakkilet *al.* catalyzed the reductive

cleavage of azo bond by an enzyme called azoreductase, which leads to disappearance of colour. However, complete mineralization of toxic by-products is not possible by the biological processes [9].

Apart from these techniques, heterogeneous photocatalysis with large band gap semiconductors such as  $TiO_2$  (3.0-3.2 eV) [10-12] has achieved greater interest due to its high photoactivity, non-toxicity, photocorrosion resistance and other physical and chemical properties [13].  $TiO_2$  has two prominent photocatalytically active phases namely anatase and rutile. Anatase is catalytically more active than rutile even though, both phases have numerous structural and functional differences. For example, rutile has to be photocatalytically active as it is having lesser bandgap (~3.0 eV) in comparison to anatase (~3.2 eV). However, the band edges, inherent band bending, high flat band potential/redox potential of anatase makes it superior over rutile [14] in photocatalytic applications. So, anatase is regarded as more photochemically active phase of Titania due to the combined effect of lower rates of recombination of charge carriers and higher surface adsorptive capacity. Therefore, most of the studies have been carried out with anatase compared to the rutile [15]. However, the efficiency is less due to high bandgap limiting the absorption to UV fraction of light only. In order to further improve the efficiency of operation several strategies very implemented such as doping, sensitizing, tuning the morphology/size etc. In this short review, we focus mainly on different mechanisms and the adopted strategies in improving the dye degradation efficiency of  $TiO_2$  based photocatalysts.

## II. PHOTO CATALYTIC DYE DEGRADATION MECHANISMS

### 2.1. Direct mechanism for dye degradation

The mechanism occurs when the dye has ability to absorb some of the visible light. When the visible light photon ( $\lambda > 400$  nm) is absorbed by the dye molecule it gets excited from ground state (dye) to its triplet excited state (dye\*). By injecting an electron into the conduction band of  $TiO_2$ , excited state dye species converted into semi-oxidised radical cations (dye<sup>+</sup>) [16]. Super oxide radical anions ( $O_2^{\cdot -}$ ) are formed by the reaction between trapped electron and dissolved oxygen, which finally results into hydroxyl radicals ( $OH^{\cdot}$ ) formation, which is responsible for the oxidation of organic compounds as shown in fig 1.

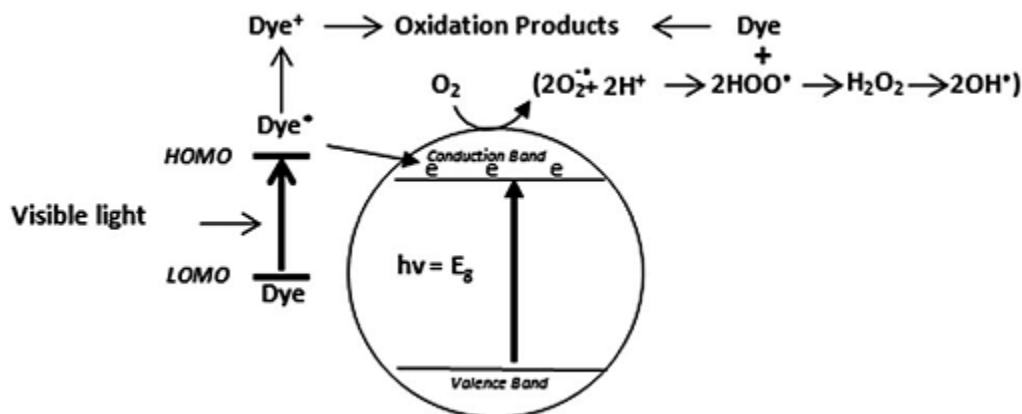
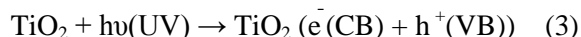


Fig 1. Representation of direct mechanism for dye degradation [17, 18]

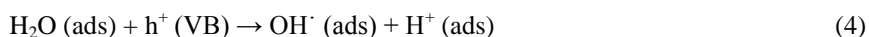
2.2. Indirect mechanism for dye degradation

Indirect mechanism using semiconducting materials can be explained by the following sequential steps [20, 21].

a. Photo excitation:When a semiconductor is irradiated with a photon ( $h\nu$ ) having energy equal to or greater than the band gap of a semiconductor (i.e.  $TiO_2$ ), photoelectron is exited from valence band to the conduction band of the semiconductor. This results in a hole and electron pair ( $e^-/h^+$ ) as shown in Eq (3).



b. Ionization of water:Hydroxyl radicals ( $OH^\cdot$ ) are formed at the valence band by the reaction between photogenerated holes and water.

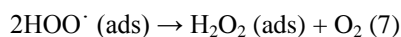


These  $OH^\cdot$  radicals are extremely powerful oxidising agents, which directly attack adsorbed organic molecules, as well as organic molecules that are close to the catalyst surface non-selectively to mineralize them upto an extent depends on their structure and stability level.

c. Oxygen ionosorption:The electron at the conduction band is taken up by the oxygen to form superoxide radical ( $O_2^{\cdot -}$ ). This superoxide radical participates in further oxidation process and also prevents the recombination of electron-hole pair and maintains electrical neutrality within the molecule. This superoxide radical formation is shown eq. (5).



d. Protonation of superoxide: Hydroxyl radicals can also produced from protonated superoxide radicalwhich can be shown by the following series of reactions.



At the surface of the photoexcited semiconductor photocatalystboth oxidation and reduction processes takes place as shown in fig 2.

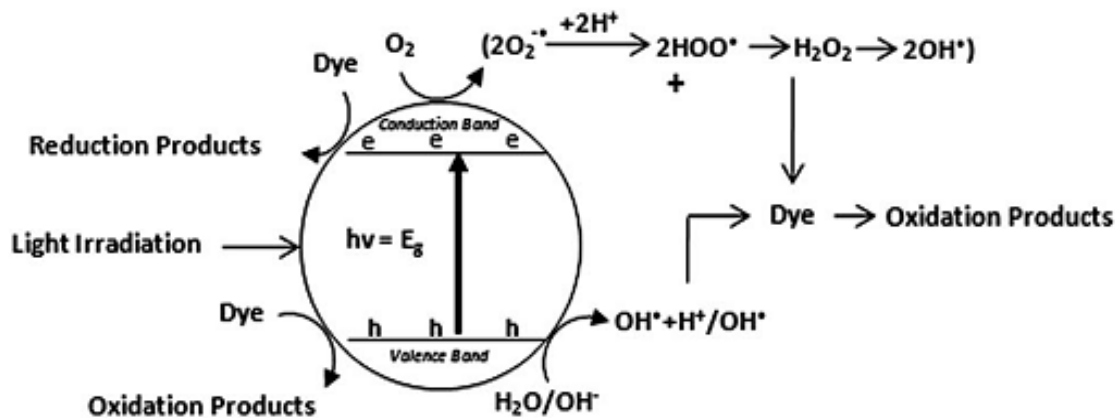


Fig2.Representation of indirectmechanism for dye degradation [19]



### III. STRATEGIES/METHODOLOGIES FOR ENHANCING TiO<sub>2</sub> PHOTOCATALYTIC PROPERTIES:

#### 3.1. Doping

Due to the band gap of TiO<sub>2</sub> (3.2eV for anatase), its photocatalytic performance is limited upto UV region only. In order to increase the performance of TiO<sub>2</sub> under visible light, the electronic structure can be modified by various doping strategies such as non-metal doping, transition metal doping, noble metal doping, lanthanide ion doping and multi-atom doping. The dopant added will improve the absorption by lowering the bandgap by forming mid gap energy states/transition energy states wherein the charge carrier life time is comparable to the original states.

##### 3.1.1 Non-metal doping

Various reports are available for enhancing TiO<sub>2</sub> performance under visible light using non-metals as dopants such as nitrogen, sulphur, carbon, boron, fluorine etc. [22, 23]. Here, we have discussed only carbon and nitrogen.

###### 3.1.1.1 Carbon doping

Both carbon and nitrogen have received more attention as dopants due to their low cost and narrow band gaps. As narrow band gaps allow them to catalyze under visible region. The routes for the synthesis of carbon doped TiO<sub>2</sub> can be broadly divided into two categories, a. inner synthetic route and b. outer synthetic route. Former includes incorporation of carbon into TiO<sub>2</sub> structure during its synthesis while later includes incorporation of carbon after TiO<sub>2</sub> has been synthesized.

Irie *et al.* synthesized carbon doped anatase TiO<sub>2</sub> nanoparticles by oxidative annealing of TiC under O<sub>2</sub> flow. During this process, temperature is maintained at 873 K [24]. Also Khan *et al.* prepared carbon doped TiO<sub>2</sub> by controlled combustion of Ti metal in a natural gas flame [25].

Renet *et al.* synthesized doped TiO<sub>2</sub> by outer synthetic route by adding required amounts of amorphous TiO<sub>2</sub>, glucose, deionized water in a Teflon lined stainless steel autoclave at 160°C for 12 hours [26].

Velmurugan *et al.* prepared carbon nanoparticle loaded TiO<sub>2</sub> (CNP-TiO<sub>2</sub>) by sonochemical method. Photocatalytic activity of CNP-TiO<sub>2</sub> under solar radiation for degradation of reactive red 120 was found to be higher than TiO<sub>2</sub> P-25 and as prepared TiO<sub>2</sub> [27]. This increased reactivity is due to the suppression in recombination of photogenerated electron-hole pairs.

###### 3.1.1.2 Nitrogen doping

Nitrogen-doped TiO<sub>2</sub> photocatalysts have been tested for decomposition of organic compounds and dyes under UV and visible light illumination [23]. Asahi *et al.* reported that nitrogen has comparable size and electronegativity to that of oxygen. Further, the O and N orbitals will intermix and narrow the bandgap. This is most suitable for reducing band gap width of TiO<sub>2</sub> [28].

Irie *et al.* proposed that in TiO<sub>2-x</sub>N<sub>x</sub> powder, an isolated narrow band is formed above the valence band, which is responsible for the visible light response [24]. Along this, if the concentration of nitrogen is increased then the quantum yield under UV is decreased which means that the doping sites could also work as recombination centres. Parida and Naik reported that the degradation efficiencies using N-doped TiO<sub>2</sub> for methylene blue and methyl orange are 67% and 59% after 4 hours irradiation under visible light source [29]. Selvaraj *et al.* reported photocatalytic degradation of various reactive triazine dyes as well as reactive yellow 84, reactive red 120,

reactive blue 160 with N-doped anatase  $\text{TiO}_2$  and P25 under natural sunlight [30]. They concluded that reactive yellow 84 fastly degraded with this N-doped  $\text{TiO}_2$  when comparing with the commercial Aeroxide P25 under sunlight. However, the photocatalytic activity of P25 is higher for the other two dyes (reactive red 120, reactive blue 160). But Ihara *et al.* and Serpone argued that during the synthesis of N-doped  $\text{TiO}_2$ , oxygen deficient sites were formed in the grain boundaries, which are responsible for the visible light response, whereas nitrogen just enhances the stabilization of these oxygen vacancies [31, 32]. Songkham and Tantirungrotechai were synthesized nitrogen and iron(III) co-doped  $\text{TiO}_2$  (N-Fe- $\text{TiO}_2$ ). They reported that N-Fe- $\text{TiO}_2$  is active for photo degradation of methyl orange [33]. Nevertheless, absorption spectra showed N-Fe- $\text{TiO}_2$  photocatalyst is only active under UV but not visible irradiation. Finally, it can be concluded that understanding of dye degradation mechanism under visible light is not clear, but still N-doped  $\text{TiO}_2$  is more important than the non-doped  $\text{TiO}_2$  in near future due to its dye degrading activity under available sunlight. Apart from advantages of non-metal doping, long-term instability of the photocatalyst is a main problem [34] which can be alleviated using transition metal doping.

### 3.1.2. Transition metal doping

Transition metals incorporation in the  $\text{TiO}_2$  crystal lattice induces a shift of light absorption towards the visible light region by forming new energy levels between valence and conduction bands. Relative energy band positions and bandwidths for anatase  $\text{TiO}_2$  of pure ( $h\nu$ ), metal-doped ( $h\nu_m$ ) and non-metal doped ( $h\nu_{nm}$ ) forms were shown in the following fig3.

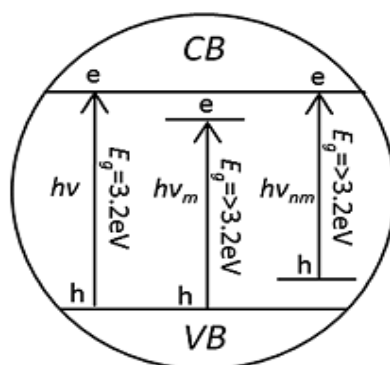


**Fig3. Representation of relative energy band positions and bandwidths for anatase  $\text{TiO}_2$  of pure ( $h\nu$ ), metal-doped ( $h\nu_m$ ) and non-metal doped ( $h\nu_{nm}$ ) forms [35].**

In this transition metal doping, cadmium and copper doping are explained in brief here.

#### 3.1.2.1. Cadmium doping

Cadmium is one of the heavy metals, which can modify the photocatalytic activity of photocatalyst (i.e.  $\text{TiO}_2$ ) by being absorbed into the photocatalyst surface. Andronic *et al.* investigated the cadmium doped  $\text{TiO}_2$  film synthesized by using doctor blade deposition method for the photocatalytic activity of methyl orange and methylene blue dyes [36]. They have been observed a linear relationship between the band gap energy of the cadmium doped  $\text{TiO}_2$  films and photo degradation efficiency of dyes. X. S. Liet *et al.* reported largely negative or no effect of cadmium ion on the photocatalytic activity [37]. Nevertheless, these effects greatly depend on the cadmium concentration and doping methods used. More studies are needed to understand the Cd system

because; it may oxidize to CdO, which modifies the electronic properties of the system, as it is a *p*-type semiconductor.

### 3.1.2.2. Copper doping

Chun *et al.* reported that Cu (II) has the ability to extend light absorption of the TiO<sub>2</sub> into visible region by modifying the TiO<sub>2</sub> valence band spectrum [38]. Andronic *et al.* have taken Cu<sub>x</sub>S and coupled Cu<sub>x</sub>S/TiO<sub>2</sub> thin films for methyl orange and methylene blue photodegradation. They reported that at Cu<sub>x</sub>S:TiO<sub>2</sub> = 3:7, along with addition of H<sub>2</sub>O<sub>2</sub>, 99% degradation efficiency is achieved for methyl orange in 300 min and methylene blue in 180 min [39].

Also, the photocatalytic activity of Cu<sub>x</sub>S/TiO<sub>2</sub> nanocomposites depends on Cu<sub>x</sub>S: TiO<sub>2</sub> ratio. Higher efficiency is due to the semiconductor association and films homogeneity limits the electron-hole recombination. Huang *et al.* tested Cu<sub>2</sub>O nanoparticles and microparticles for photo degradation of methyl orange. Cu<sub>2</sub>O nanoparticles are stable in ambient atmosphere whereas microparticles are stable as Cu<sub>2</sub>O/CuO core structure. Due to this, slow photocorrosion occurs with this Cu<sub>2</sub>O microparticles. However, Cu<sub>2</sub>O microparticles showed higher photocatalytic activity for methyl orange than that of its nanoparticles because; nanoparticles are deactivated during the photo catalytic reaction [40]. However, transition doping may cause thermal instability for the anatase phase of TiO<sub>2</sub>.

### 3.1.3. Lanthanide ions doping

Lanthanide ions are recognized due to their complex formation with the Lewis bases such as acids, amines, alcohols, aldehydes etc. as these bases interact with the f-orbital of the lanthanides through their functional groups. Therefore, inclusion of lanthanide ions into the TiO<sub>2</sub> matrix could provide a good contact between the organic pollutants to the surface of the semiconductor. Hence, enhances the photoactivity of TiO<sub>2</sub> [41]. Recent studies explained La<sup>3+</sup>, Nd<sup>3+</sup>, Sm<sup>3+</sup>, Eu<sup>3+</sup>, Gd<sup>3+</sup> and Yb<sup>3+</sup> modified TiO<sub>2</sub> nanoparticles have ability to increase the stability of anatase phase. Xie *et al.* synthesized three types of lanthanide ion-modified TiO<sub>2</sub> such as Nd<sup>3+</sup>-TiO<sub>2</sub>, Eu<sup>3+</sup>-TiO<sub>2</sub>, Ce<sup>3+</sup>-TiO<sub>2</sub> and tested for photo degradation of azo dye X-3B under visible light irradiation [42]. They ranked the reaction rates as Nd<sup>3+</sup>-TiO<sub>2</sub> sol > Eu<sup>3+</sup>-TiO<sub>2</sub> sol > Ce<sup>3+</sup>-TiO<sub>2</sub> sol > TiO<sub>2</sub> sol > P25 TiO<sub>2</sub> powder.

Zhang *et al.* prepared TiO<sub>2</sub> particles co-doped with boron and lanthanum (B-La-TiO<sub>2</sub>) at 1:4 molar ratios. Its degradation efficiency for methyl orange is 98% in 90 min and 24% for undoped TiO<sub>2</sub>. The reason for this efficiency is due to its tremendous photocatalytic effect under visible light region [43]. Lanet *et al.* synthesized lanthanum and boron co-doped TiO<sub>2</sub> (La-B-TiO<sub>2</sub>) by modified sol-gel method. 1% La-B-TiO<sub>2</sub> catalyst showed 93% degrading efficiency for acid orange 7 under visible light irradiation in 5 hours.

Nasiret *et al.* prepared 0.1 Ce/C co-doped TiO<sub>2</sub> through hydrothermal method for effective acid orange 7-dye degradation under visible light. Co-doped catalysts showed better activity than C-doped catalyst. However, increase in the concentration of Ce above 0.1 Ce/C-TiO<sub>2</sub> increased the electrons and holes recombination [44]. They finally concluded that, surface hydroxyl groups are increased abundantly due to increase in the surface area as the particle size is decreased and electron-hole recombination is reduced. Both of these enhanced the photocatalytic degradation of acid orange dye.

### 3.1.4. Noble metal doping

TiO<sub>2</sub> modified with noble metal exhibits excellent stability and reproducibility. Several studies have been reported that noble metal modified catalyst acts as an electron trap due to the formation of schottky barrier thus reduces the recombination of electron-hole pairs, thereby photocatalytic efficiency is improved [45]. Most recent work is going with the silver and platinum doped TiO<sub>2</sub>, in which silvermodified TiO<sub>2</sub> is explained in detail below.

Gupta *et al.* synthesized silver-doped TiO<sub>2</sub>, they were regenerated the Ag<sup>+</sup> doped TiO<sub>2</sub> by washing the catalyst with distilled water thoroughly. The degradation efficiency is achieved by Ag<sup>+</sup> doped TiO<sub>2</sub> is >99% for basic violet 3 and methyl red in 90 min along with 86% mineralization efficiency [46]. Seery *et al.* reported that increase in decolourization of rhodamine 6 G with Ag modified TiO<sub>2</sub> is due to increase in the visible absorption capacity of silver nanoparticles [47]. However, there is need to increase the optical properties. For this, some potential transition metals are used to tailor the band gap width of TiO<sub>2</sub>/Ag<sub>2</sub>O [48].

### 3.2. Dye sensitization

Since dyes have absorption in the visible part of the solar spectrum, dye sensitization will be helpful due to adsorption and subsequent hot electron transfer from the surface of dye to the surface of TiO<sub>2</sub>, and improve the efficiency [49]. Dye sensitized degradation is mainly aided by enhanced adhesion of the dye molecule on the surface of TiO<sub>2</sub> in the presence of oxygen which can easily look for the injected electrons from the conduction band.

Zhang *et al.* reported that aerobic selective oxidation of alcohols is achieved by an anthraquinonic dye (alizarin red S) sensitized TiO<sub>2</sub> and a nitroxyl radical (2, 2, 6, 6-tetramethyl-piperidinyloxy). The mechanism mainly involves the formation of a dye radical cation that oxidizes the nitroxyl radical. This radical species is mainly responsible for the oxidation of alcohols into aldehydes [50]. Conjugated polymers such as polyaniline and polythiophene can also be used as TiO<sub>2</sub> sensitizers for the dye degradation.

### 3.3. Graphene modified TiO<sub>2</sub>

Graphene is an atomic sheet of sp<sup>2</sup>-bonded carbon atoms with unique properties such as high conductivity, high transparency due to its one-atom thickness and large specific surface area.

Zhang *et al.* synthesized P25-graphene composite by hydrothermal method. During the process, graphene oxide is reduced to graphene and then P25 nanoparticles were deposited onto the graphene sheet. P25-graphene composite is more active than P25 for the degradation of methylene blue due to reduced recombination of the charge and increased absorptivity [51]. Furthermore, TiO<sub>2</sub>/graphene composites have been well studied as an electrode material and solar light photocatalyst for the lithium-ion batteries.

### 3.4. Structurally modified TiO<sub>2</sub>

To increase the activity of photocatalyst, different shapes of TiO<sub>2</sub> were employed such as nanoparticles, nanotubes, nanorods, nanorings, nanosheets, nanocombs, nanobelt etc. The photocatalytic activity of TiO<sub>2</sub> nanotubes is strongly influenced by tube diameter and thickness. If the tube thickness increases, then degradation efficiency increases until a maximum value is reached but again decreases to a steady value.



Compared to anatase or P25 TiO<sub>2</sub>nanoparticulate films, nanotube arrays with similar thickness and geometric area are more active. The increased dye degradation activity is due to effective separation of electron-hole pairs, which takes place in a ordered way in TiO<sub>2</sub>nanoarray film and also due to higher internal surface area of the nanotube structure [52].

### 3.5. Fullerenes modified TiO<sub>2</sub>

Fullerene is a molecule entirely composed of carbon. They have many different forms, from which spherical fullerenes are called as buckyballs. Cylindrical forms are named as carbon nanotubes or buckytubes. Krishna *et al.* have taken polyhydroxy fullerenes (PHF) to enhance the photocatalytic efficiency of TiO<sub>2</sub> for the procion red dye [53]. Electrostatic forces adsorb PHF molecules on the surface of TiO<sub>2</sub>. This enables scavenging of photogenerated electrons that result in decreasing the charge recombination.

## IV. SPECIAL CASES IN TiO<sub>2</sub> PHOTOCATALYSIS:

Even though, several strategies have been employed for improving the photo/catalytic efficiency, only limited performance is achieved with TiO<sub>2</sub> based photocatalysts in dye degradation studies as the photocatalysis is a complex heterogeneous chemical reaction. Therefore, several unaddressed issues in this area which need to be explored. Firstly, the form of photocatalyst that taken for dye degradation studies plays an important role as the kinetics have major impact on charge carrier recombination rate. For ex: if the catalyst is in the form of coating then there is no need to perform post filtration and centrifugation. Nevertheless, this reduces efficiency of the system due to loss of exposed surface area. Secondly, if the catalyst is in powder form, the problems regarding this are stirring should perform during operation and collection of the catalyst from the treated water after every run. . Further, one has to take into account the stability of dye before or during degradation studies, as some times dye itself degrade utilising the fraction of light illuminated without photocatalyst. In this section, we discuss methods for fixing the TiO<sub>2</sub> on supporting materials such as activated carbon, silica, zeolite etc to alleviate the existing problems as well as to limit the usage of photocatalysts.

### 4.1. TiO<sub>2</sub> on zeolite support

Zeolites are the aluminosilicate members of microporous solids known as molecular sieves. They provide effective electric field of their framework for the charge separation. Mathews *et al.* reported that the OH<sup>·</sup> radicals produced on the surface of the TiO<sub>2</sub> could be easily transferred to the zeolite surface as shown in the fig4. Thus enhanced efficiency of dye degradation [55]

### 4.2. Silica as TiO<sub>2</sub> support

Recently, amorphous SiO<sub>2</sub> has become useful because of its high adsorption capacity. Presence of more number of acid sites and hydroxyl groups on amorphous SiO<sub>2</sub>, it has good absorptive properties. Hence, it is used as TiO<sub>2</sub> support.

Sun *et al.* investigated the catalytic properties of three porous amorphous silica for rhodamine B. They concluded that nature of silica supports could affect the particle size and crystal form of TiO<sub>2</sub>. Opal and porous supported



photocatalysts ( $\text{TiO}_2/\text{SiO}_2$ ) showed better catalytic performance of 85% decolourization for rhodamine B at different calcination temperatures [56].

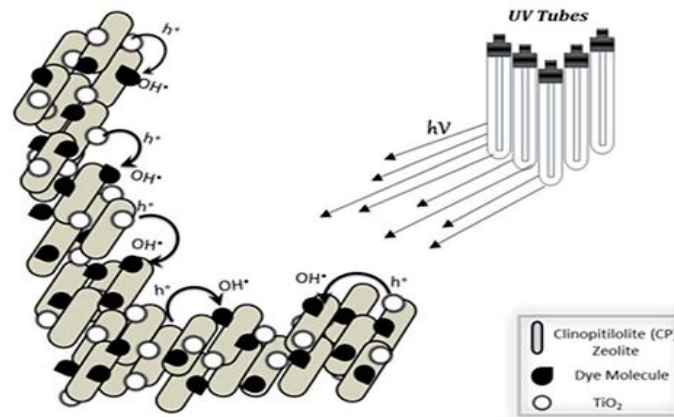


Fig 4.Enhanced charge separation in the zeolite supported  $\text{TiO}_2$  [57].

#### 4.3. $\text{TiO}_2$ on activated carbon support

Activated carbon also known as activated charcoal which is highly porous form of carbon with pore ranges as macro(wavelength > 50 nm), meso (0.5-1  $\mu\text{m}$ ) and micro (<1 $\mu\text{m}$ ). Dye removal by adsorption using activated carbon is the common method and used as a support for most heterogeneous catalysis reactions [58].

Activated carbon performance mainly depends on type of carbon used and characteristics of the aqueous solution containing various chemical contaminants. Like other dye removal treatments, activated charcoal is suitable for one particular type of pollutant and ineffective on other. Even though, activated carbon is expensive but it comes with the advantage of regeneration.

Activated carbon supported  $\text{TiO}_2$  allow more contact between reactants and  $\text{TiO}_2$ .So that they easily formed into intermediate compounds which is shown in fig5. Zhang *et al.* proposed similar design regarding AC supported  $\text{TiO}_2$ . However, the band gap tuning of  $\text{TiO}_2$  is not achieved by the Activated carbon.

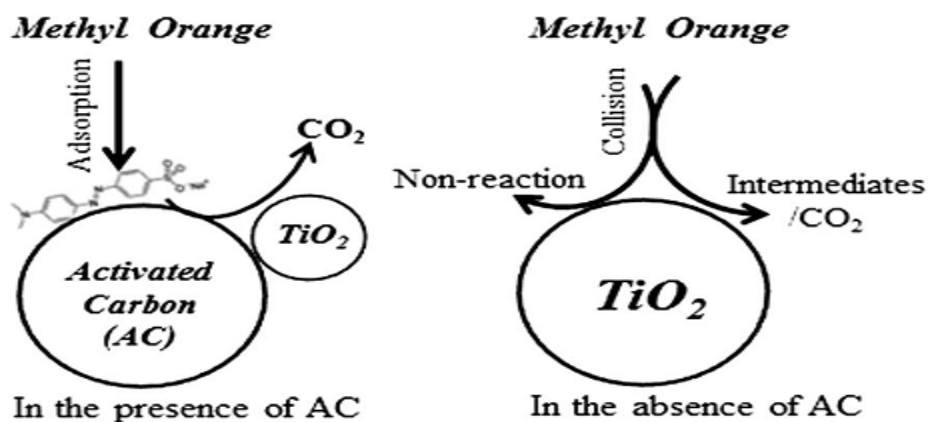


Fig5.Methyl orange degradation mechanism with AC- $\text{TiO}_2$  composites [59].

#### 4.4. Carbon nanotubes as TiO<sub>2</sub> supports

Researchers have more interest towards carbon nanotubes as they possess unique electronic properties. They are explained simply as rolled graphene sheet. There are two types of nanotubes i.e. single walled carbon nanotubes (SWCNTs) and multi walled carbon nanotubes (MWCNTs). CNTs have high surface-to-volume ratio, which is the main property to use it for the degradation of dyes. Yu *et al.* compared the effect of MWCNTs on the adsorption and the photocatalytic properties of TiO<sub>2</sub> P-25. They reported that, mixture of CNTs and TiO<sub>2</sub> showed improved activity for the treatment of three azo dyes compared to the activity by activated carbon [60]. The short MWCNTs are used initial materials for the fabrication of TiO<sub>2</sub>/short MWCNTs nanocomposites, which were tested for photodegradation of reactive brilliant red X-3B. Thus, various photocatalysts were ranked as TiO<sub>2</sub>/short MWCNTs > TiO<sub>2</sub>/MWCNTs > TiO<sub>2</sub> > P-25.

#### 4.5 TiO<sub>2</sub> coupled with semiconductors

The Victoria charge transfer from one semiconductor to another with suitable band edge positions that is thermodynamically favourable can increase the lifetime of the charge carriers thus promoting the interfacial charge transfer and catalytic efficiency [61]. Coupling the TiO<sub>2</sub> with a wide band gap semiconductor like SnO<sub>2</sub> is reported to enhance the charge separation and thus the photocatalytic activity. The CB edges of anatase TiO<sub>2</sub> and SnO<sub>2</sub> are situated at 0.34 and +0.07 V, respectively, while the VB edge of SnO<sub>2</sub> (+3.67 V) is much more positive than that of anatase TiO<sub>2</sub> (+2.87 V) as shown in Fig 6.

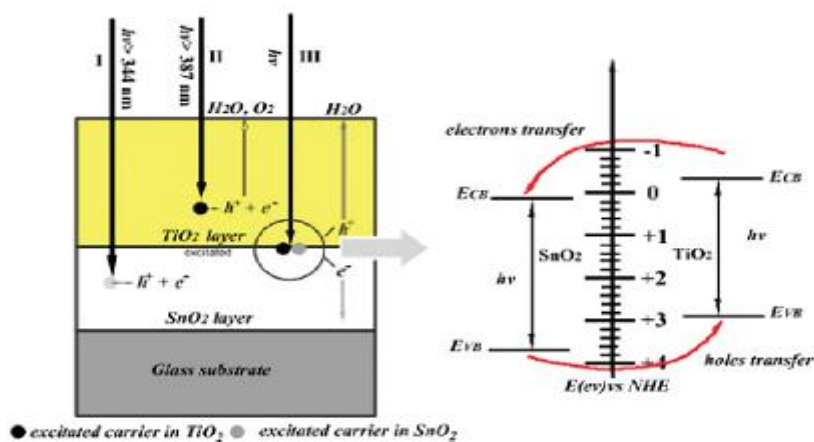
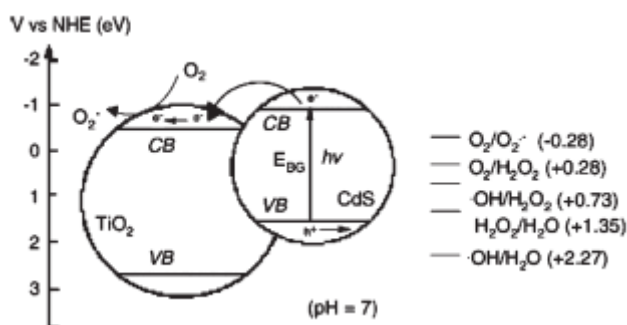


Fig 6. Representation of the interfacial charge transfer processes in the SnO<sub>2</sub>-TiO<sub>2</sub> composite film [62]

The SnO<sub>2</sub>-TiO<sub>2</sub> composite films fabricated on transparent electro-conductive glass substrates showed superior activity for the degradation of Rhodamine B (RhB) due to the combined effects of low sodium content, better crystallization, appropriate phase composition of anatase (73.4%) and rutile (26.3%), and slower recombination rate of charge carriers [62]. However, the activity of large band gap semiconductors limits to UV region only. Therefore, the formation of heterojunction structure between a narrowband gap semiconductor and TiO<sub>2</sub> with matching band potentials provides an effective way to extend the photosensitivity of TiO<sub>2</sub> to the visible portion of the solar spectrum.



Wu *et al.* reported that the direct formation of nanocrystalline TiO<sub>2</sub> coupled with highly dispersed CdS nanocrystal at low temperature by a combined micro emulsion and solvothermal method resulted in the faster degradation of methylene blue (MB) under visible light irradiation [63]. ESR results revealed that the electrons from the excited CdS were injected into the titania CB and then were scavenged by molecular oxygen to yield a superoxide radical anion in oxygen-equilibrated media, which is shown in fig 7.



**Fig 7. Redox potentials of the VB and CB of CdS sensitized TiO<sub>2</sub> nanoparticles and various redox processes occurring on their surface at pH 7 [63]**

## V. CONCLUSION

TiO<sub>2</sub> is an important semiconducting material for photo catalysis/dye degradation studies owing to its stability, abundant availability in a nut shell, though it has inherent surface characteristics. Several strategies of improving the efficiencies are reported in this area. However, significant research still is possible as this is a complex heterogeneous chemical reaction. In this review article, different mechanism, strategies of improving the efficiency is discussed thoroughly. Further one need to look into deeper aspects of molecular mechanisms on catalyst surface which helps to simplify the analysis of catalyst-photon interaction.

## VI. ACKNOWLEDGEMENTS

We sincerely acknowledge Head of the department, department of Chemical engineering, JNTUCEA, Ananthapuram for providing resource facilities in writing this short review article. Further, we take this opportunity to acknowledge lab members of our group in getting the information and help to complete this draft in time.

## REFERENCES

1. Y. M. Slokar and A. Majcen Le Marechal, *Dyes Pigm.*, 1998, 37, 335–356.
2. M. Sleiman, D. Vildoza, C. Ferronato and J.-M. Chovelon, *Appl. Catal., B*, 2007, 77, 1–11.
3. W. Kuo, *Water Res.*, 1992, 26, 881–886.
4. N. Ince and D. Gönöncü, *Environ. Technol.*, 1997, 18, 179–185.
5. O. Tunay, I. Kabdasli, G. Eremektar and D. Orhon, *Water Sci. Technol.*, 1996, 34, 9–16.
6. M. Saquib and M. Muneer, *Dyes Pigm.*, 2003, 56, 37–49.
7. E. P. Reddy, L. Davydov and P. Smirniotis, *Appl. Catal., B*, 2003, 42, 1–11.

8. O. J. Hao, H. Kim and P.-C. Chiang, *Crit. Rev. Environ. Sci. Technol*, 2000, 30, 449–505.
9. A. Moutaouakkil, Y. Zeroual, F. ZohraDzayri, M. Talbi, K. Lee and M. Blaghen, *Arch. Biochem. Biophys*, 2003, 413, 139–146.
10. M. Stylidi, D. I. Kondarides and X. E. Verykios, *Appl. Catal., B*, 2004, 47, 189–201.
11. S. Kaur and V. Singh, *J. Hazard. Mater*, 2007, 141, 230–236.
12. C. Kormann, D. Bahnemann and M. R. Hoffmann, *Environ. Sci. Technol.*, 1991, 25, 494–500.
13. P. Pizarro, C. Guillard, N. Perol and J.-M. Herrmann, *Catal. Today*, 2005, 101, 211–218.
14. D. C. Hurum, A. G. Agrios, K. A. Gray, T. Rajh and M. C. Thurnauer, *J. Phys. Chem. B*, 2003, 107, 4545–4549.
15. V. K. Gupta, R. Jain, A. Nayak, S. Agarwal and M. Shrivastava, *Mater. Sci. Eng., C*, 2011, 31, 1062–1067.
16. S. Sreekantan and L. C. Wei, *J. Alloys Compd.*, 2010, 490, 436–442.
17. H.-F. Yu and S.-T. Yang, *J. Alloys Compd.*, 2010, 492, 695–700.
18. M. A. Fox and M. T. Dulay, *Chem. Rev.*, 1993, 93, 341–357.
19. J. Zhao, C. Chen and W. Ma, *Top. Catal.*, 2005, 35, 269–278.
20. M. R. Hoffmann, S. T. Martin, W. Choi and D. W. Bahnemann, *Chem. Rev.*, 1995, 95, 69–96.
21. J. Peral, X. Domenech and D. F. Olliss, *J. Chem. Technol. Biotechnol.*, 1997, 70, 117–140.
22. M. Fittipaldi, V. Gombac, A. Gasparotto, C. Deiana, G. Adami, D. Barreca, T. Montini, G. Martra, D. Gatteschi and P. Fornasiero, *ChemPhysChem*, 2011, 12, 2221–2224.
23. D. Chen, Z. Jiang, J. Geng, Q. Wang and D. Yang, *Ind. Eng. Chem. Res.*, 2007, 46, 2741–2746.
24. H. Irie, Y. Watanabe and K. Hashimoto, *J. Phys. Chem. B*, 2003, 107, 5483–5486.
25. S. U. Khan, M. Al-Shahry and W. B. Ingler, *science*, 2002, 297, 2243–2245.
26. W. Ren, Z. Aia, F. Jia, L. Zhanga, X. Fanb and Z. Zoub, *Appl. Catal., B*, 2007, 69, 138–144.
27. R. Velmurugan, B. Krishnakumar, B. Subash and M. Swaminathan, *Sol. Energy Mater. Sol. Cells*, 2013, 108, 205–212.
28. R. Asahi, T. Morikawa, T. Ohwaki, K. Aoki and Y. Taga *science*, 2001, 293, 269–271.
29. K. Parida and B. Naik, *J. Colloid Interface Sci.*, 2009, 333, 269–276.
30. A. Selvaraj, S. Sivakumar, A. Ramasamy and V. Balasubramanian, *Res. Chem. Intermed.*, 2013, 39, 2287–2302.
31. T. Ihara, M. Miyoshi, Y. Iriyama, O. Matsumoto and S. Sugihara, *Appl. Catal., B*, 2003, 42, 403–409.
32. N. Serpone, *J. Phys. Chem. B*, 2006, 110, 24287–24293.
33. P. Songkhum and J. Tantirungrotechai, *Res. Chem. Intermed.*, 2013, 39, 1555–1561.
34. Y. Zhang, H. Xu, Y. Xu, H. Zhang and Y. Wang, *J. Photochem. Photobiol., A*, 2005, 170, 279–285.
35. A. Zaleska, *Recent Pat. Eng.*, 2008, 2, 157–164.
36. L. Andronic, A. Enesca, C. Vladuta and A. Duta, *Chem. Eng. J.*, 2009, 152, 64–71.
37. X. S. Li, G. E. Fryxell, M. H. Engelhard and C. Wang, *Inorg. Chem. Commun.*, 2007, 10, 639–641.
38. H. Chun, T. Yuchao and T. Hongxiao, *Catal. Today*, 2004, 90, 325–330.
39. L. Andronic, L. Isac and A. Duta, *J. Photochem. Photobiol., A*, 2011, 221, 30–37.
40. L. Huang, F. Peng, H. Yu and H. Wang, *Solid State Sci.*, 2009, 11, 129–138.

41. K. Ranjit, I. Willner, S. Bossmann and A. Braun, *Environ. Sci. Technol.*, 2001, 35, 1544–1549.
42. Y. Xie, C. Yuan and X. Li, *Colloids Surf, A*, 2005, 252, 87–94.
43. W. Zhang, X. Li, G. Jia, Y. Gao, H. Wang, Z. Cao, C. Li and J. Liu, *Catal. Commun.*, 2014, 45, 144–147.
44. M. Nasir, J. Zhang, F. Chen and B. Tian, *Res. Chem. Intermed.*, 2013, 1–18.
45. M. K. Seery, R. George, P. Floris and S. C. Pillai, *J. Photochem. Photobiol., A*, 2007, 189, 258–263.
46. A. Gupta, A. Pal and C. Sahoo, *Dyes Pigm.*, 2006, 69, 224–232.
47. M. K. Seery, R. George, P. Floris and S. C. Pillai, *J. Photochem. Photobiol., A*, 2007, 189, 258–263.
48. S. T. Hussain, Rashid, D. Anjum, A. Siddiqi and A. Badshah, *Mater. Res. Bull.*, 2013, 48, 705–714.
49. S. Kaur and V. Singh, *J. Hazard. Mater.*, 2007, 141, 230–236.
50. M. Zhang, C. Chen, W. Ma and J. Zhao, *Angew. Chem.*, 2008, 120, 9876–9879.
51. H. Zhang, X. Lv, Y. Li, Y. Wang and J. Li, *ACS Nano*, 2009, 4, 380–386.
52. H.-F. Zhuang, C.-J. Lin, Y.-K. Lai, L. Sun and J. Li, *Environ. Sci. Technol.*, 2007, 41, 4735–4740.
53. V. Krishna, N. Noguchi, B. Koopman and B. Moudgil, *J. Colloid Interface Sci.*, 2006, 304, 166–171.
54. N. Bao, X. Feng, Z. Yang, L. Shen and X. Lu, *Environ. Sci. Technol.*, 2004, 38, 2729–2736.
55. R. W. Matthews, *J. Catal.*, 1988, 111, 264–272.
56. Z. Sun, C. Bai, S. Zheng, X. Yang and R. L. Frost, *Appl. Catal., A*, 2013, 458, 103–110.
57. M. Nikazar, K. Gholivand and K. Mahanpoor, *Desalination*, 2008, 219, 293–300.
58. F. Rodriguez-Reinoso, *Carbon*, 1998, 36, 159–175.
59. X. Zhang, M. Zhou and L. Lei, *Carbon*, 2005, 43, 1700–1708.
60. Y. Yu, J. C. Yu, C.-Y. Chan, Y.-K. Che, J.-C. Zhao, L. Ding, W.-K. Ge and P.-K. Wong, *Appl. Catal., B*, 2005, 61, 1–11.
61. Serpone, N.; Borgarello, E.; Gratzel, M.J. *Chem. Soc., Chem. Commun.* 1984, 342–344.
62. Zhou, M.; Yu, J.; Liu, S.; Zhai, P.; Jiang, L.J. *Hazard. Mater.* 2008, 154, 1141–1148.
63. Wu, L.; Yu, J. C.; Fu, X.J. *Mol. Catal. A: Chem.* 2006, 244, 25–32.